ISBN 978-989-9121-59-1
57th LISBON Global Congress on "Chemical, Biological, Environment & Medical Sciences" (LCBEM-25)
Dec. 10-12, 2025 Lisbon (Portugal)

Recovery of Metals from Waste PCBs Using Acid-Salt Synergistic Dissolution

Mihlali Dyanty[1], Lukhanyo Mekuto[2], Elvis Fosso-Kankeu[1]

[1]Department of Metallurgy, Doornfontein Campus, University of Johannesburg, P.O. Box 17011, Johannesburg 2028, South Africa
[2]Department of Chemical Engineering, Doornfontein Campus, University of Johannesburg, P.O. Box 17011, Johannesburg 2028, South Africa

Abstract: *This study addressed the growing challenge of electronic waste and the drawbacks of conventional hydrometallurgical processes, which often rely on hazardous reagents. It investigated a more sustainable approach for metal recovery from printed circuit boards (PCBs) by comparing three leaching systems: sulfuric acid (H_2SO_4), H_2SO_4 –$Fe_2(SO_4)_3$, and H_2SO_4 –$(NH_4)_2S_2O_8$. Using Response Surface Methodology to assess the effects of temperature (25–65 °C) and time (15–480 min), the ammonium persulfate system emerged as the most efficient. It achieved near-complete copper recovery (up to 100%), significantly surpassing the other systems. In contrast, silver recovery remained low (<35%) across all conditions, confirming its refractory behaviour within PCB material. Statistical analysis showed that dissolution time strongly influenced copper extraction, while temperature had minimal impact. Overall, the H_2SO_4 –$(NH_4)_2S_2O_8$ system demonstrated high efficiency under mild conditions, highlighting its potential as a more environmentally friendly alternative to traditional leaching methods.*

Keywords: *Ammonium Persulphate, Copper, Ferrous Sulphate, Leaching, Printed Circuit Boards, Silver*

I. Introduction

The rapid accumulation of electronic waste (e-waste) has drawn increasing attention, as it is considered the fastest growing residue globally [5]. With an annual growth rate exceeding 70 million tons [5, 9], this rise is driven by technological advancements and the short life spans of devices such as cell phones and computers [4, 10]. E-waste originates from household appliances, communication devices, and electronic gadgets [10], and although hazardous, it represents a valuable secondary resource for base metals and precious metals [3, 4, 14]. Printed circuit boards (PCBs), which contain the majority of these valuable metals [3], include various electronic components that require dismantling and multiple separation steps before processing [10, 14]. Metal recovery routes such as mechanical, hydrometallurgical, and pyrometallurgical processes are widely used [4, 9] but often unsustainable due to high costs, energy demands, and pollution [10]. Bio-metallurgy offers an alternative but remains limited by insufficient data and poorly defined operating conditions [10]. Hydrometallurgy is considered the most suitable method because of its high selectivity, adaptability, and predictable performance [4, 11]. Traditional leaching agents which include aqua regia, cyanide, nitric acid, thiourea, and hydrochloric acid are effective but toxic, unstable, and environmentally harmful [2, 4, 10]. Acid–salt synergy, where combined reagents outperform individual components [7], has been explored using salts such as ferric sulphate, ammonium sulphate, and cupric chloride [11, 13], though their application to PCBs remains limited. This study investigates the synergistic leaching behaviour of sulfuric acid (H_2SO_4) with ferrous sulphate ($Fe_2(SO_4)_3$) and ammonium persulfate ($(NH_4)_2S_2O_8$) for PCB metal recovery. Three different systems, namely: H_2SO_4, H_2SO_4 –

$Fe_2(SO_4)_3$, and H_2SO_4 –$(NH_4)_2S_2O_8$ are compared using response surface methodology. The study focuses specifically on silver and copper extraction from PCBs.

2. Methodology

2.1. Chemicals and Equipment

Sulfuric acid (H_2SO_4), ferrous sulphate ($Fe_2(SO_4)_3$), ammonium persulfate ($(NH_4)_2S_2O_8$), hydrogen peroxide (H_2O_2), deionized water, hydrochloric acid, and nitric acid were used throughout the study. The equipment included conical flasks, 250 mL glass beakers, an analytical balance, standard sieves, a pulveriser, cutting tools, a cutting mill or rotary disc mill, and a rotary divider. A fume hood and a hot plate with a magnetic stirring, or alternatively a temperature-controlled water bath, were used for sample handling and heating. Analytical techniques included atomic absorption spectroscopy (AAS), X-ray fluorescence (XRF), and scanning electron microscopy with Energy-Dispersive X-ray Spectroscopy (SEM-EDS).

2.2. PCB Sample Preparation

Printed circuit boards (PCBs) were manually cut into 2 × 2 cm pieces and subjected to further size reduction using a rotary disc mill (or cutting mill) for six cycles of 30 seconds each. Plastics and low-density materials were removed using water separation based on density differences. Thermal pre-treatment was then carried out in an oven at 700 °C for 5 hours to eliminate remaining plastics and organic components, as described by [9]. Magnetic materials were manually removed with a magnet, and the remaining fraction was thoroughly mixed to ensure homogeneity. The bulk material was then split using a rotary divider to obtain representative samples for head-grade analysis.

2.3. Characterization of Material

Characterization was conducted at the University of Johannesburg's metallurgy analytical laboratory (Doornfontein Campus). X-ray fluorescence spectroscopy (XRF, Rigaku ZSX Primus II) and scanning electron microscopy equipped with energy dispersive spectroscopy (SEM-EDS, Tescan), were used to determine elemental composition, particle distribution, and surface morphology.

2.4. Head Sample Analysis Using Aqua Regia

A representative sample collected from the rotary splitter was subjected to acid digestion. Aqua regia was prepared at a ratio of 25% HCl to 75% HNO_3 in a 500 mL glass beaker, and 8 g of the PCB sample was added. Digestion was performed under a fume hood at room temperature for 3 hours to ensure complete dissolution of metallic components. The solution was then filtered to obtain the leach liquor, which was analysed using AAS to determine metal concentrations.

2.5. Dissolution Tests

Dissolution experiments were carried out using response surface methodology (RSM). A central composite design (CCD) was used to evaluate the influence of temperature and time on the selective recovery of silver and copper. The independent variables and their coded levels are presented in Table 1. The response variables were the percentage recovery of silver and copper, measured by AAS following each experimental run. RSM was used to model the relationship between the independent variables and metal recovery, allowing prediction of optimal operating conditions. The experimental matrix generated by CCD included thirteen runs for each leaching system, as summarised in Table 2. With three systems tested, a total of 39 runs were completed, 78 runs when duplicates were included.

TABLE 1. EXPERIMENTAL LEVELS AND CODE FOR CCD.

			Coded levels		
Symbol	Variables	Unit	-1	0	1
X_1	Temperature	°C	25	45	65
X_2	Time	min	15	247,5	430

TABLE II. EXPERIMENTAL RUN TABLE – METAL RECOVERY USING ALL THREE SYSTEMS.

StdOrder	RunOrder	PtType	Blocks	Temperature	Time
11	1	0	1	25	247,5
13	2	0	1	45	247,5
6	3	-1	1	65	15,0
1	4	1	1	45	15,0
8	5	-1	1	25	480,0
12	6	0	1	45	247,5
3	7	1	1	65	247,5
2	8	1	1	65	480,0
4	9	1	1	45	247,5
9	10	0	1	45	247,5
5	11	-1	1	25	15,0
7	12	-1	1	45	247,5
10	13	0	1	45	480,0

2.6. Experimental Setup

Leaching was performed in 250 mL conical flasks, each containing 8 g of PCB sample. Three leaching systems were prepared: H_2SO_4 alone, H_2SO_4 with $Fe_2(SO_4)_3$, and H_2SO_4 with $(NH_4)_2S_2O_8$. For each run, 250 mL of the prepared leaching solution was added, and 13 mL of H_2O_2 was introduced within the first 5 minutes to initiate dissolution and enhance metal solubilization. The mixtures were placed in an incubator and agitated at 160 rpm to ensure uniform contact between solids and reagents. At the end of each run, the mixtures were filtered to separate solids from the pregnant leach solution. The filtrates were analysed using atomic absorption spectroscopy (AAS, Thermo-Scientific iCE 3000 series) to determine silver and copper concentrations for recovery calculations.

3. Results and Discussion

3.1.Characterization of PCB Sample

XRF analysis, shown in Table 3, revealed that iron was the most abundant metal in the PCB sample, followed by copper, with additional base metals such as zinc, lead, and nickel also present. Precious metals including gold and silver were not detected by XRF due to their extremely low concentrations. The XRF data was consistent with findings reported by [8, 13], apart from detecting any traces of gold and silver. SEM imaging, in Figure 1, showed a heterogeneous particle surface, with bright regions corresponding to metallic components embedded within a non-metallic matrix. These non-metallic particles, largely composed of silica, provide structural support to the metallic layers, as described by [6]. Elemental mapping using SEM–EDS, shown in Table 5, confirmed the presence of metals such as nickel, iron, zinc and copper, along with trace amounts of platinum. Although gold and silver were not detected by EDS, aqua regia digestion (head-grade analysis) confirmed the presence of silver at 10.65 mg/L and copper at 1790.75 mg/L, demonstrating that the precious metals were present in quantities too low for detection by XRF and EDS but recoverable through chemical dissolution.

TABLE III. COMPOSITION OF PCBS FROM XRF ANALYSIS.

Element	Fe	Cu	Br	Al	Zn	Pb	Ni	Si
PCB sample composition (%)	11.06	9.3	6.8	4.5	4.3	3.6	1.2	6,08

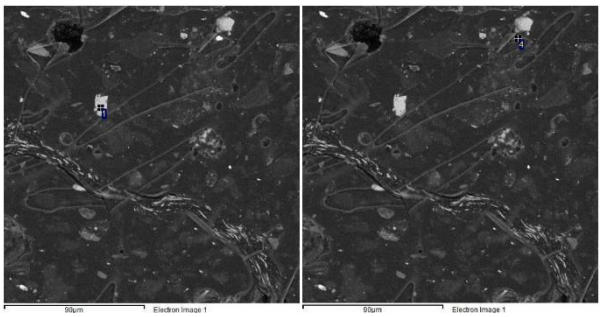

Fig. 1. SEM analysis of the PCB sample.

TABLE IV. COMPOSITION OF THE PCB SAMPLE FROM EDS ANALYSIS.

Element	Fe	Al	Ni	Zn	Pt	Cu
PCB sample composition (%)	7.48	7.31	0.61	0.47	0.29	0.1

3.2.Leaching Behaviour of Silver and Copper

The role of temperature and dissolution time was investigated using RSM. Figures 2 and 3 summarise the dissolution trends for both metals across all systems.

3.3.Effect of Temperature

Temperature had minimal influence on silver recovery, with the highest extraction observed at 45 °C, while copper dissolution was highest at 25 °C, as seen in Figures 2 and 3. Across all systems, especially in the ammonium persulfate system, the effect of temperature was weak, indicating that leaching was not temperature-dependent within the studied range. This aligns with [12], who reported that persulfate-based leaching efficiency is governed primarily by oxidant concentration and that higher temperatures reduce persulfate ion stability. The ammonium persulfate system consistently produced higher recoveries than both the ferrous sulphate and acid-only systems.

3.4.Effect of Time

Reaction time had a more pronounced influence on dissolution. For silver, as seen in Figure 2, recovery generally increased with time before declining, suggesting oxidant depletion or re-precipitation at prolonged durations. This pattern was observed for both salt-containing systems. In the acid-only system, silver recovery increased steadily at 25 °C but decreased at higher temperatures. Copper, demonstrated a continuous increase in recovery with time across all systems, as seen in Figure 3, reaching maximum dissolution at 480 minutes. Time was therefore identified as the dominant variable for copper extraction. Among the three systems, ammonium persulphate again produced greater recoveries, while the acid-only and ferrous sulphate systems displayed similar behaviour.

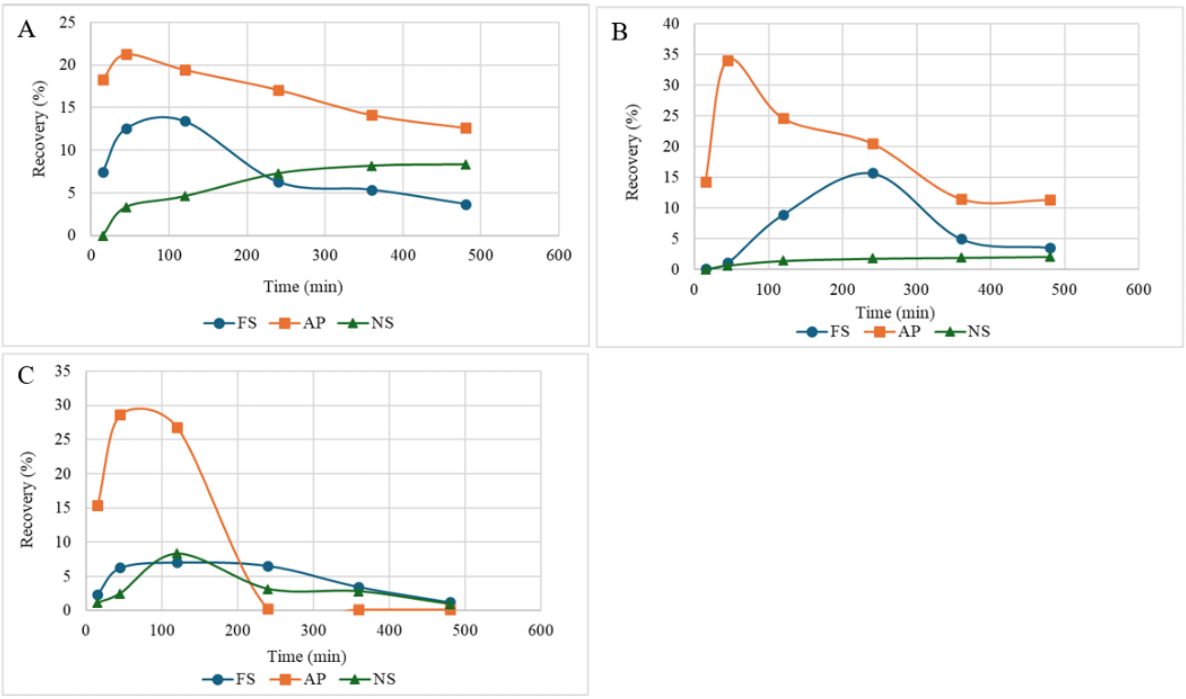

Fig. 2. Recovery plots for Ag recovery for each system at over time at different temperature (A). 25 ℃, (B). 45 ℃ and (C). 65 ℃.

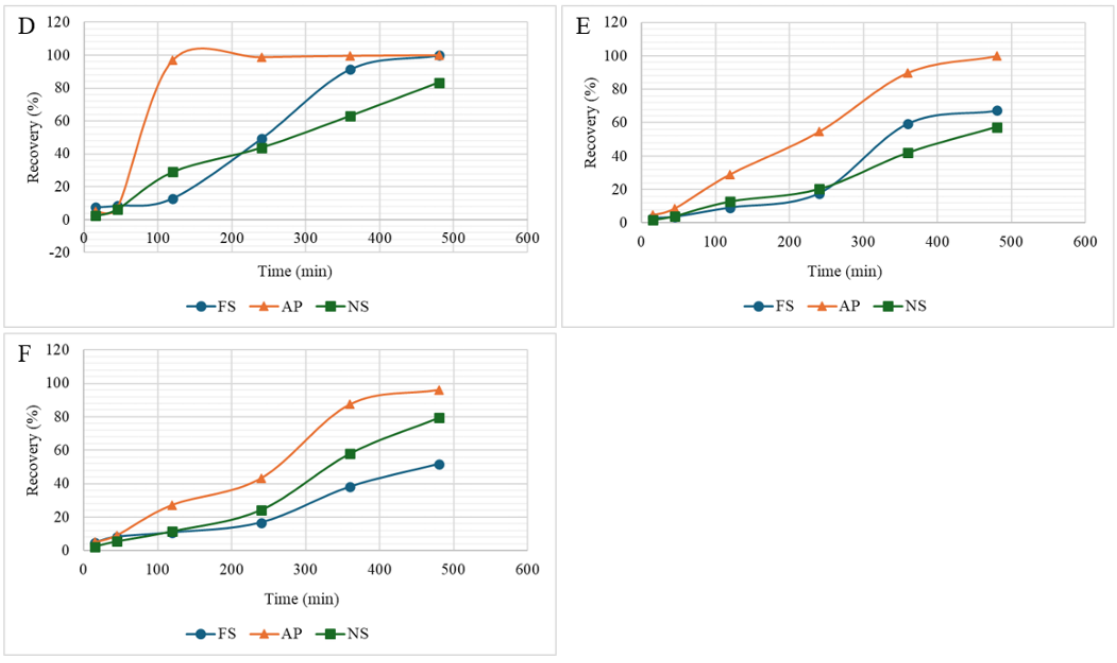

Fig. 3. Recovery plots for Cu recovery for each system over time at different temperature (D). 25 ℃, (E). 45 ℃ and (F). 65 ℃.

3.5. Model Fitting and Statistical Analysis

RSM using a Central Composite Design (CCD) was used to evaluate the effects of temperature (X_1) and time (X_2). Six mathematical models corresponding to each response, were generated for the three systems as shown in Table 5 and Equations 1–6. The ANOVA results, shown in Tables 6 – 11, indicated that the overall models were statistically significant at a 95% confidence interval ($P < 0.05$), with large F-values confirming model adequacy. From the ANOVA results, the P – value is obtained,

this is used to identify the components affecting the recovery of silver and copper [1]. The P- value has to be below 0.05. For K_1, X_2^2 had a P – value 0.008, this means that it had an influence on the recovery of silver. This is also evident for K_2 and K_3 in which X_1 (with a P – value of 0.017) and X_2 and X_1^2 (with P - values of 0.017 and 0.004) influenced the recovery of silver respectively. For copper, for K_4, X_1, X_2, X_1^2, X_2^2 had P – values of 0, 0, 0.001 and 0.001 respectively. For K_5, X_2 had a P – value of 0, whilst for K_6, X_2 and X_1^2 have P – values of 0 and 0.012. This means that they had an influence on the responses [1]. Model accuracy was further confirmed by the coefficient of determination (R^2). As shown in Figure 4 and Table 14, copper models (K_4 , K_5 , K_6) demonstrated excellent correlation between actual and predicted values, with R^2 values of 0.9911, 0.924, and 0.9682 respectively. Silver models (K_1 , K_2 , K_3) showed good correlations, with R^2 values of 0.7854, 0.7993 0.873 respectively, which is sufficient for trend prediction within the experimental domain.

TABLE V. SYMBOLS FOR EACH RESPONSE.

Responses	Symbol
FS-Acid (Ag Recovery %)	K_1
APS-Acid (Ag Recovery %)	K_2
Acid (Ag Recovery %)	K_3
FS-Acid (Cu Recovery %)	K_4
APS-Acid (Cu Recovery %)	K_5
Acid (Cu Recovery %)	K_6

$$K_1 = -10{,}8 + 0{,}787\,X_1 + 0{,}0704\,X_2 - 0{,}00980\,X_1^2 - 0{,}000157\,X_2^2 + 0{,}000139\,X_1 X_2 \quad (1)$$

$$K_2 = -7{,}2 + 1{,}369\,X_1 + 0{,}0294\,X_2 - 0{,}01677\,X_1^2 - 0{,}000047\,X_2^2 - 0{,}000516\,X_1 X_2 \quad (2)$$

$$K_3 = -43{,}1 + 2{,}144\,X_1 + 0{,}0851\,X_2 - 0{,}02352\,X_1^2 - 0{,}000090\,X_2^2 - 0{,}000460\,X_1 X_2 \quad (3)$$

$$K_4 = 56{,}2 - 2{,}522\,X_1 + 0{,}1380\,X_2 + 0{,}02702\,X_1^2 + 0{,}000238\,X_2^2 - 0{,}002441\,X_1 X_2 \quad (4)$$

$$K_5 = 56{,}2 - 2{,}28\,X_1 + 0{,}3080\,X_2 + 0{,}0204\,X_1^2 - 0{,}000196\,X_2^2 - 0{,}00021\,X_1 X_2 \quad (5)$$

$$K_6 = 64{,}4 - 3{,}062\,X_1 + 0{,}0841\,X_2 + 0{,}03243\,X_1^2 + 0{,}000159\,X_2^2 - 0{,}000215\,X_1 X_2 \quad (6)$$

TABLE VI. ANOVA FOR QUADRATIC MODEL FOR K1.

	Analysis of Variance					
	Source	Degrees of Freedom	Sum of squares	Mean square	F-Value	P-Value
K1	Model	5	375,431	75,086	5,13	0,027
	Linear	2	9,217	4,609	0,31	0,74
	X1	1	8,857	8,857	0,6	0,462
	X2	1	0,36	0,36	0,02	0,88
	Square	2	364,537	182,268	12,44	0,005
	X1*X1	1	42,459	42,459	2,9	0,132
	X2*X2	1	199,119	199,119	13,59	0,008
	2-Way Interaction	1	1,677	1,677	0,11	0,745
	X1*X2	1	1,677	1,677	0,11	0,745
	Error	7	102,555	14,651		
	Lack-of-Fit	3	102,555	34,185		
	Pure Error	4	0	0		

TABLE VII. ANOVA FOR QUADRATIC MODEL FOR K2.

	Analysis of Variance					
	Source	Degrees of Freedom	Sum of squares	Mean square	F-Value	P-Value
K2	Model	5	499,849	99,97	5,58	0,022
	Linear	2	268,382	134,191	7,49	0,018
	X_1	1	173,021	173,021	9,65	0,017
	X_2	1	95,361	95,361	5,32	0,054
	Square	2	208,475	104,237	5,81	0,033
	X_1*X_1	1	124,301	124,301	6,93	0,034
	X_2*X_2	1	17,94	17,94	1	0,35
	2-Way Interaction	1	22,992	22,992	1,28	0,295
	X_1*X_2	1	22,992	22,992	1,28	0,295
	Error	7	125,487	17,927		
	Lack-of-Fit	3	125,487	41,829		
	Pure Error	4	0	0		

TABLE III. ANOVA FOR QUADRATIC MODEL K_3.

	Analysis of Variance					
	Source	Degrees of Freedom	Sum of squares	Mean square	F-Value	P-Value
K3	Model	5	638,971	127,794	9,62	0,005
	Linear	2	145,77	72,885	5,49	0,037
	X_1	1	18,166	18,166	1,37	0,28
	X_2	1	127,605	127,605	9,61	0,017
	Square	2	474,882	237,441	17,88	0,002
	X_1*X_1	1	244,418	244,418	18,41	0,004
	X_2*X_2	1	65,295	65,295	4,92	0,062
	2-Way Interaction	1	18,318	18,318	1,38	0,279
	X_1*X_2	1	18,318	18,318	1,38	0,279
	Error	7	92,957	13,28		
	Lack-of-Fit	3	92,957	30,986		
	Pure Error	4	0	0		

TABLE IX. ANOVA FOR QUADRATIC MODEL K_4.

	Analysis of Variance					
	Source	Degrees of Freedom	Sum of squares	Mean square	F-Value	P-Value
K4	Model	5	9851,49	1970,3	156,49	0
	Linear	2	8080,55	4040,28	320,9	0
	X_1	1	1158,15	1158,15	91,99	0
	X_2	1	6922,41	6922,41	549,81	0
	Square	2	1255,65	627,82	49,86	0
	X_1*X_1	1	322,58	322,58	25,62	0,001
	X_2*X_2	1	457,99	457,99	36,38	0,001
	2-Way Interaction	1	515,29	515,29	40,93	0
	X_1*X_2	1	515,29	515,29	40,93	0
	Error	7	88,13	12,59		
	Lack-of-Fit	3	88,13	29,38		
	Pure Error	4	0	0		

TABLE 2. ANOVA FOR QUADRATIC MODEL K_5.

	Analysis of Variance					
	Source	Degrees of Freedom	Sum of squares	Mean square	F-Value	P-Value
K5	Model	5	14146,9	2829,4	17,02	0,001
	Linear	2	13779,2	6889,6	41,45	0
	X_1	1	588,1	588,1	3,54	0,102
	X_2	1	13191,1	13191,1	79,37	0
	Square	2	363,9	182	1,09	0,386
	X_1*X_1	1	183,1	183,1	1,1	0,329
	X_2*X_2	1	309,4	309,4	1,86	0,215
	2-Way Interaction	1	3,8	3,8	0,02	0,884
	X_1*X_2	1	3,8	3,8	0,02	0,884
	Error	7	1163,4	166,2		
	Lack-of-Fit	3	1163,4	387,8		
	Pure Error	4	0	0		

TABLE 3. ANOVA FOR QUADRATIC MODEL K_6.

	Analysis of Variance					
	Source	Degrees of Freedom	Sum of squares	Mean square	F-Value	P-Value
K_6	Model	5	8761,02	1752,2	42,57	0
	Linear	2	7700,32	3850,16	93,53	0
	X_1	1	91,89	91,89	2,23	0,179
	X_2	1	7608,43	7608,43	184,83	0
	Square	2	1056,72	528,36	12,84	0,005
	X_1*X_1	1	464,83	464,83	11,29	0,012
	X_2*X_2	1	203,94	203,94	4,95	0,061
	2-Way Interaction	1	3,98	3,98	0,1	0,765
	X_1*X_2	1	3,98	3,98	0,1	0,765
	Error	7	288,15	41,16		
	Lack-of-Fit	3	288,15	96,05		
	Pure Error	4	0	0		

TABLE XII. ACTUAL VS PREDICTED RESPONSES FOR AG RECOVERY FOR EACH RESPONSE.

K_1	K_1 - Predicted	K_2	K_2 - Predicted	K_3	K_3 - Predicted
6,28	11,46	17,01	17,69	7,29	8,45
15,70	14,16	20,51	19,03	16,72	16,12
2,37	0,13	15,40	10,79	1,13	-2,36
0,11	5,92	14,26	20,47	0,00	6,65
3,68	2,07	12,64	13,55	8,35	10,34
15,70	14,16	20,51	19,03	16,72	16,12
6,52	9,03	0,24	6,95	3,15	4,97
1,21	0,94	0,12	-1,98	0,92	2,58
15,70	14,16	20,51	19,03	16,72	16,12
15,70	14,16	20,51	19,03	16,72	16,12
7,43	3,86	18,33	16,73	0,00	-3,16
15,70	14,16	20,51	19,03	16,72	16,12
3,55	5,43	11,31	12,50	19,53	15,87

TABLE XIII. ACTUAL VS PREDICTED RESPONSES FOR CU RECOVERY FOR EACH RESPONSE.

K_4	K_4 - Predicted	K_5	K_5 - Predicted	K_6	K_6 - Predicted
49,27	43,65	98,75	74,94	43,74	37,39
17,65	18,95	54,52	56,90	20,31	20,50
4,77	6,12	4,95	-1,36	2,32	3,55
2,94	-2,14	4,67	-0,57	1,80	-6,51
99,95	101,84	99,96	112,22	83,33	82,59
17,65	18,95	54,52	56,90	20,31	20,50
16,73	15,86	43,24	55,14	24,19	29,56
51,84	51,36	96,07	90,47	79,37	72,77
17,65	18,95	54,52	56,90	20,31	20,50
17,65	18,95	54,52	56,90	20,31	20,50
7,48	11,21	4,95	16,50	2,29	9,38
17,65	18,95	54,52	56,90	20,31	20,50
67,20	65,79	99,87	93,21	57,37	64,71

TABLE XIV. R_2 AND ADJUSTED R2 FOR EACH RESPONSE OBTAINED FROM ANOVA.

	R^2	Adj R^2
K_1	0,7854	0,6322
K_2	0,7993	0,656
K_3	0,873	0,7823
K_4	0,9911	0,9848
K_5	0,924	0,8697
K_6	0,9682	0,9454

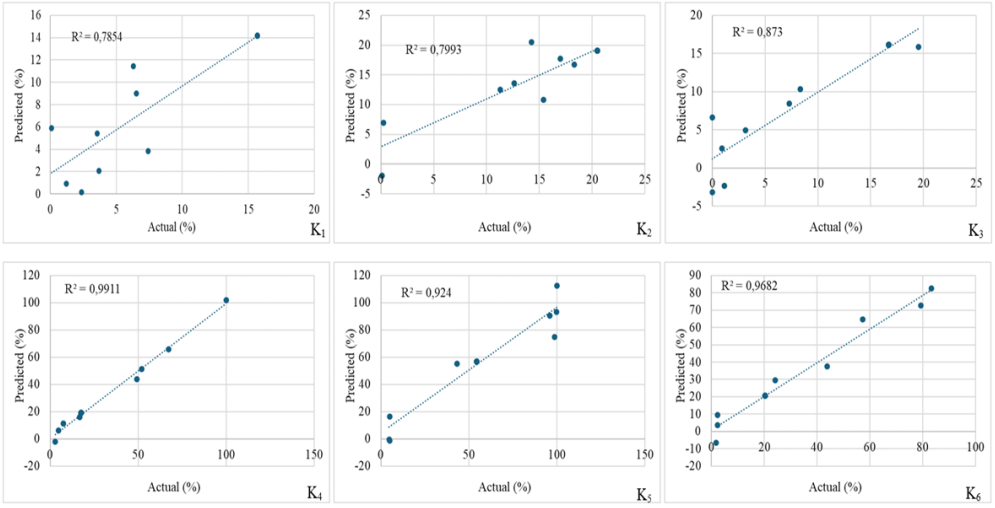

Fig. 4. Experimental values vs Predicted values for each response.

3.6. Response Plots and Interaction Effects

Contour plots, found in Figures 5 and 6, illustrated the interactions between temperature and time. For silver, K_1 displayed negligible interaction effects, as shown by circular contour patterns, indicating that neither temperature nor time strongly influenced recovery within the tested range. K_2 was moderately temperature-sensitive, while K_3 was predominantly influenced by time. Copper contour plots displayed negligible temperature influence for all systems, with elongated contour shapes indicating that time was the primary controlling factor for dissolution efficiency. No significant interaction between temperature and time was observed.

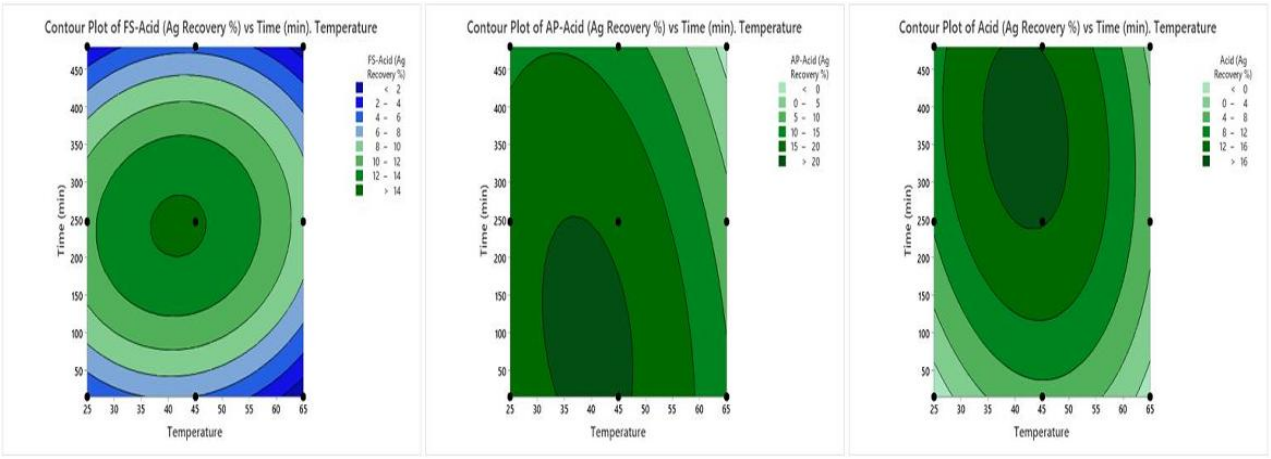

Fig. 5. Contour plots between variables for silver for each response.

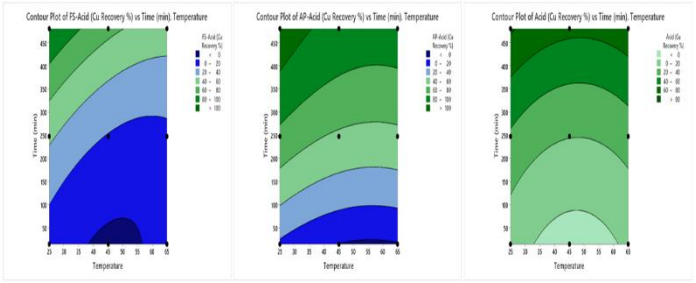

Fig. 6. Contour plots between variables for copper for each response.

3.7. Optimal Leaching Conditions

Since silver recoveries were low, with a maximum of 34.1%, optimization for silver was not pursued. As seen in Figure 7, for copper, RSM predicted clear optimal conditions for each system. For K_4 , a maximum recovery of 100% was predicted at 25.79 °C and 480 minutes. For K_5 , optimal recovery (100%) was obtained at 26.2 °C and 398.7 minutes. For K_6 , the model predicted an optimal recovery of 82.6% at 25 °C and 480 minutes. Due to the limited availability of PCB sample material, confirmation experiments could not be performed.

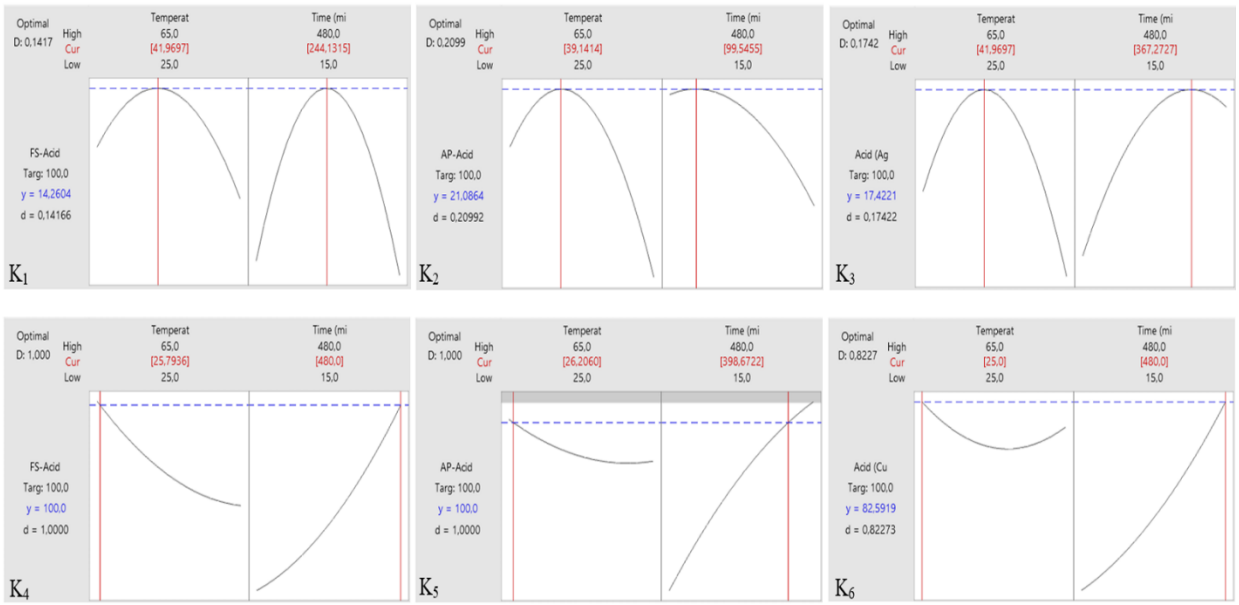

Fig. 7. Optimization results for each response and system.

4. Conclusion

This study evaluated the acid–salt synergy of H_2SO_4, H_2SO_4 –$Fe_2(SO_4)_3$, and H_2SO_4 –$(NH_4)_2S_2O_8$ for leaching metals from waste PCBs. The H_2SO_4 –$(NH_4)_2S_2O_8$ system showed the strongest synergistic effect, achieving the highest copper recovery and outperforming the other two systems. RSM confirmed that dissolution time was the key variable influencing copper leaching, while temperature had little effect, allowing efficient extraction at near-room-temperature conditions. Silver recovery remained consistently low (maximum 34.1%), indicating that the selected lixiviants were ineffective for breaking down its complex binding within PCBs. Although XRF and EDS did not detect precious metals, aqua regia digestion confirmed their presence. Overall, the H_2SO_4 –$(NH_4)_2S_2O_8$ system is highly effective for copper recovery, but alternative leaching strategies are required for silver. Future work should test silver-specific lixiviants such as thiourea, thiosulfate, or chloride-based systems [13] and perform confirmatory experiments to validate the RSM predictions.

5. Acknowledgement

The authors are grateful for the financial support received from the Faculty of Engineering and The Built Environment at the University of Johannesburg in South Africa.

6. References

[1] Abdol Jani, W. N. F., Suja', F., Sayed Jamaludin, S. I., Mohamad, N. F., & Abdul Rani, N. H. (2023). Optimization of Precious Metals Recovery from Electronic Waste by Chromobacterium violaceum Using Response Surface Methodology (RSM). Bioinorganic Chemistry and Applications, 2023. https://doi.org/10.1155/2023/4011670

[2] Alzate, A., López, M. E., & Serna, C. (2016). Recovery of gold from waste electrical and electronic equipment (WEEE) using ammonium persulfate. Waste Management, 57, 113 120. https://doi.org/10.1016/j.wasman. 2016.01.043

[3] Barrueto, Y., Hernández, P., Jiménez, Y. P., & Morales, J. (2022). Properties and application of ionic liquids in leaching base/precious metals from e-waste. A review. In Hydrometallurgy (Vol. 212). https://doi.org/10.1016/j.hydromet.2022.105895

[4] Chen, M., Huang, J., Ogunseitan, O. A., Zhu, N., & Wang, Y. min. (2015). Comparative study on copper leaching from waste printed circuit boards by typical ionic liquid acids. Waste Management, 41, 142–147. https://doi.org/10.1016/j.wasman.2015.03.037

[5] Domańska, U., Wiśniewska, A., & Dąbrowski, Z. (2024). Recovery of Strategic Metals from Waste Printed Circuit Boards with Deep Eutectic Solvents and Ionic Liquids. Processes, 12(3).

https://doi.org/10.3390/pr12030530
[6] Godigamuwa, K., & Okibe, N. (2023). Gold Leaching from Printed Circuit Boards Using a Novel Synergistic Effect of Glycine and Thiosulfate. Minerals, 13(10). https://doi.org/10.3390/min13101270
[7] Jaffe, K. (n.d.). The Scientific Roots of Synergy and how to make cooperation successful. https://ssrn.com/abstract=4682310
[8] Kahar, I. N. S., Othman, N., Noah, N. F. M., & Suliman, S. S. (2023). Recovery of copper and silver from industrial e-waste leached solutions using sustainable liquid membrane technology: a review. In Environmental Science and Pollution Research (Vol. 30, Issue 25, pp. 66445–66472). Springer Science and Business Media Deutschland GmbH. https://doi.org/10.1007/s11356-023-26951-0
[9] Łukomska, A., Wiśniewska, A., Dąbrowski, Z., Lach, J., Wróbel, K., Kolasa, D., & Domańska, U. (2022). Recovery of Metals from Electronic Waste-Printed Circuit Boards by Ionic Liquids, DESs and Organophosphorous-Based Acid Extraction. Molecules, 27(15). https://doi.org/10.3390/molecules27154984
[10] Oke, E. A., & Potgieter, H. (2024). Recent chemical methods for metals recovery from printed circuit boards: A review. In Journal of Material Cycles and Waste Management (Vol. 26, Issue 3, pp. 1349–1368). Springer. https://doi.org/10.1007/s10163-024-01944-4
[11] Pinho, S. C., Ribeiro, C., Ferraz, C. A., & Almeida, M. F. (2021). Copper, zinc, and nickel recovery from printed circuit boards using an ammonia–ammonium sulphate system. Journal of Material Cycles and Waste Management, 23(4), 1456–1465. https://doi.org/10.1007/s10163-021-01226-3.
[12] Tuncuk, A. (2019). Lab scale optimization and two-step sequential bench scale reactor leaching tests for the chemical dissolution of Cu, Au & Ag from waste electrical and electronic equipment (WEEE). Waste https://doi.org/10.1016/j.wasman. 2019.07.008 the Management, 95, 636–643.
[13] Yazici, E. Y., & Deveci, H. (2014). Ferric sulphate leaching of metals from waste printed circuit International Journal of Mineral Processing, 133, 39–45. https://doi.org/10.1016/j.minpro. 2014.09.015
[14] Zhu, P., Chen, Y., Wang, L. Y., & Zhou, M. (2012). Treatment of waste printed circuit board by green solvent using ionic liquid. Waste Management, 32(10), 1914–1918. https://doi.org/10.1016/j.wasman. 2012.05.025